

# Patch clamp investigation into the phosphate carrier from *Saccharomyces cerevisiae* mitochondria

Klaus Herick, Reinhard Krämer, Hinrich Lühning \*

Institut für Biotechnologie I, Institut für Biologische Informationsverarbeitung I, Forschungszentrum Jülich GmbH, D-52425 Jülich, Germany

Received 26 February 1997; revised 1 May 1997; accepted 13 May 1997

## Abstract

After heterologous expression in *E. coli*, functionally active phosphate carrier (PIC) from *Saccharomyces cerevisiae* mitochondria was purified and reconstituted into giant liposomes and used for patch clamp experiments. Single channel currents across excised patches revealed an anion channel function of the PIC protein. Besides the three transport modes known to date, namely phosphate/phosphate exchange, phosphate/ $\text{OH}^-$  exchange and mercurial-induced unidirectional transport, this channel activity represents the fourth transport mode of the PIC. The PIC channel activity was sensitive towards phosphate as its physiological substrate. Phosphate (10 mM) blocked in a specific but reversible manner the PIC channel, suggesting a phosphate-dependent conformational change of the protein into the carrier mode. Furthermore, the current through the channel and its gating activity were affected by divalent cations. In the presence of  $\text{Ca}^{2+}$  and  $\text{Mg}^{2+}$ , the channel displayed a mean conductance of  $25 \pm 5$  pS whereas  $40 \pm 10$  pS was observed in the absence of divalent cations. Also, the dwell times in either the open or closed state of the PIC channel appeared to be prolonged in the presence of  $\text{Ca}^{2+}$  and  $\text{Mg}^{2+}$ . The observed PIC channel characteristics are discussed with respect to previously reported electrophysiological in situ measurements on anion channels of the inner mitochondrial membrane. Similarities of the PIC channel to the inner mitochondrial anion channel (IMAC) have been found. © 1997 Elsevier Science B.V.

**Keywords:** Ion channel; Phosphate carrier; Mitochondrion; (*Saccharomyces cerevisiae*)

## 1. Introduction

Solute transport across the inner mitochondrial membrane is mediated by a family of highly specific transport proteins (for review see [1,2]). One of these proteins, the phosphate carrier (PIC), is involved in the mitochondrial energy metabolism by providing with inorganic phosphate the matrix space for ATP synthesis [3–5]. Functional properties of the PIC have been investigated using intact mitochondria as well as reconstituted systems [1,3,5]. Three transport

Abbreviations: AAC, ATP/ADP carrier;  $\text{C}_{12}\text{E}_8$ , octaethylglycol-monododecylether; DTE, 1,4-dithioerythritol; EDTA, ethylenediaminetetraacetic acid;  $\text{KP}_i$ ,  $\text{K}_2\text{HPO}_4/\text{KH}_2\text{PO}_4$ ; MES, 2-[*N*-morpholino]ethane-sulfonic acid;  $\text{P}_i$ , inorganic phosphate; PIC, phosphate (inorganic) carrier; PIPES, (piperazine-*N,N'*-[2-ethanesulfonic acid]); SDS–PAGE, sodium dodecylsulfate polyacrylamide gel electrophoresis; SLS, sodium lauroylsarcosinate; Tris, tris(hydroxymethyl)aminomethane; UCP, uncoupling protein

\* Corresponding author. Fax: +49-2461-614216.

modes of the PIC protein have been observed: (i) Homologous phosphate/phosphate exchange, (ii) phosphate/ $\text{OH}^-$  exchange (i.e., physiologically productive net phosphate transport) and (iii) a unidirectional transport after modification by mercurials [5]. This fully reversible mercurial-induced uniport mode has been found for several mitochondrial carriers [6,7]. It is characterized by both carrier-like and channel-like properties. Although the translocation rate of these transporters appeared to be low ( $< 100 \text{ s}^{-1}$ , see [8]), and thus a function as ion channel can hardly be ascribed to those carriers, recent electrophysiological measurements revealed the channel function of the nucleotide carrier and the uncoupling protein [9,10]. Previously, the chloroplast triosephosphate/phosphate carrier has been shown to act as a channel protein under certain conditions [11].

Here, we report a fourth transport mode of the mitochondrial phosphate carrier, using heterologously expressed PIC protein. The carrier displays  $\text{Cl}^-$  channel behavior that is specifically blocked by phosphate, but not by sulfate, vanadate, or ADP. The *mir* gene encoding the phosphate carrier from *Saccharomyces cerevisiae* was overexpressed in *E. coli* [12]. Inclusion bodies formed in this strain were solubilized and purified [13]. The active PIC protein was reconstituted into giant liposomes and examined with patch clamp techniques. By this procedure, we could exclude contamination by any other mitochondrial protein. This is the first time that electrophysiological data are presented showing that the overexpressed phosphate translocator in a highly purified state without contaminations may also act as an ion channel. This information significantly adds to previous publications of reconstituted carriers which also showed channel-like function.

## 2. Materials and methods

### 2.1. Chemicals

[ $^{33}\text{P}$ ]phosphate was obtained from Amersham-Buchler. Sigma supplied the following chemicals: Triton X-100, cardiolipin sodium salt, mersalylic acid, DTE, PIPES, azolectin and turkey egg yolk phospholipid. Dowex 2-X10, soybean phosphatidylcholine and sodium lauroylsarcosinate (SLS) were purchased from

Fluka, Bio-Beads SM-2 from Bio-Rad, Sephadex G-75 from Pharmacia and pyridoxalphosphat from Merck. All other chemicals were of analytical grade. Azolectin was purified by acetone precipitation [14].

### 2.2. Isolation and purification of the PIC

The gene coding for the PIC was cloned from a yeast genomic library as described earlier [15] and the PIC was expressed in the *E. coli* strain BL21(DE3) [12,13,16]. The expression strain BL21(DE3) was transformed with the plasmid coding for the wilde type PIC. The expression was carried out as follows: A total of 1 l of  $2 \times \text{YT}$  medium (plus 100 mg of carbenicillin) was inoculated with a fresh overnight colony of transformed BL21(DE3) cells and grown to an absorbance of 0.6 at 600 nm wavelength (about 5 h,  $37^\circ\text{C}$ ) under vigorous shaking. Expression of PIC was initiated by the addition of 1 mM isopropyl- $\beta$ -D-thiogalactopyranoside and 100 mg carbenicillin. Growth was continued for 3 h, then the cells were harvested and stored at  $-20^\circ\text{C}$ . The following steps were carried out at  $4^\circ\text{C}$ . The pellet containing cells from 125 ml of the cell culture was resuspended in Tris-EDTA buffer (10 mM Tris base, 0.1 mM EDTA, 1 mM DTE, adjusted to pH 7.0 with NaOH) and passed twice through a french pressure cell (16000 psi, large cell), followed by centrifugation at  $12000 \times g$  for 10 min. The pellet was homogenized with 10 ml of Tris-EDTA buffer and centrifuged at  $1100 \times g$  for 5 min, the supernatant was centrifuged at  $12000 \times g$  for 3 min. The final pellet was stored at  $-20^\circ\text{C}$ . Purification of the PIC from isolated inclusion bodies was carried out similar to the protocol employed for the oxoglutarate carrier [17] and for the phosphate carrier [13,18]. The pellet was resuspended 3 times in Tris-EDTA buffer containing 2% Triton X-100, followed by centrifugation at  $12100 \times g$  for 2.5 min. The supernatant was discarded. Eventually, the pellet was solubilized in 500  $\mu\text{l}$  Tris-EDTA buffer containing 1.67% SLS, and 1 ml of  $\text{H}_2\text{O}$  was added. 200  $\mu\text{l}$  (0.7 to 1 mg) of the solubilized protein was incubated for 30 min in 0.6% Triton X-100, 50 mM KCl, 20 mM  $\text{KP}_i$  pH 6.5, and then transferred to a hydroxyapatite column (400 mg, pasteur pipette,  $4^\circ\text{C}$ ). Five fractions of 500  $\mu\text{l}$  were collected using an elution buffer containing 0.6% Triton X-100, 50 mM KCl, 20 mM  $\text{KP}_i$ , 1 mM DTE

and 0.4 mg ml<sup>-1</sup> cardiolipin, pH 6.5. All fractions were analyzed by SDS–PAGE, and fractions 2 to 5 were used for reconstitution.

### 2.3. Preparation of proteoliposomes

The solubilized PIC was reconstituted into preformed phospholipid vesicles according to the amberlite method which had been established for the PIC from bovine heart mitochondria [5]. Since an increased population density of PIC in the giant liposomes was necessary to detect single transport molecules by patch clamp technique, the original purification procedure had been slightly modified. A phospholipid concentration of 16 mg ml<sup>-1</sup> was used at a phospholipid/protein ratio of 250 (w/w) and a detergent/phospholipid ratio of 0.79 (w/w). A detergent/biobeads ratio of 12 mg/g in combination with 15 column passages was used to remove the detergent Triton X-100. Proteoliposomes were formed using sonicated egg yolk phosphatidylcholine (16 mg ml<sup>-1</sup>) and additional cardiolipin (0.23 mg ml<sup>-1</sup>) in a solution composed of 50 mM PIPES pH 6.5 and 30 mM KP<sub>i</sub> for tracer experiments. For patch clamp experiments, purified soybean phosphatidylcholine (16 mg ml<sup>-1</sup>) and cardiolipin (0.23 mg ml<sup>-1</sup>) in 50 mM MES–Tris pH 7.4 and 100 mM KCl were used.

### 2.4. Measurement of transport activity

The P<sub>i</sub>/P<sub>i</sub> antiport activity of the reconstituted PIC was determined by measuring the import of [<sup>33</sup>P]phosphate into the vesicles [5]. Briefly, the reconstituted PIC was inhibited by 100 μM mersalyl and the external P<sub>i</sub> was replaced by an isoosmolar concentration of sucrose during a size exclusion chromatography on Sephadex G-75 columns. A precedent inhibition of PIC by mersalyl was accomplished to prevent phosphate net transport [5]. Transport was started by addition of 10 mM DTE and 5 mM labeled phosphate, simultaneously, to the proteoliposomes, thereby reverting the mersalyl-induced inhibition. Using the inhibitor stop technique, 40 mM pyridoxalphosphate were added to terminate the transport assay [5]. Finally, each sample was passed through an anion exchange column (Dowex 1-X8, chloride form) in order to remove the external radioactivity. The exchange rates were determined as described elsewhere [5].

### 2.5. Protein determination

The protein concentrations were determined according to the modified Lowry method after precipitation with deoxycholate and trichloroacetic acid, and extraction of detergent and lipid with organic solvents [19,20].

### 2.6. Preparation of giant liposomes

For the preparation of giant liposomes, a modified method of dehydration and rehydration according to Criado and Keller was used [11,21]. Proteoliposomes containing 100 mM KCl and 50 mM MES–Tris pH 7.4 were mixed with one to three volumes of sonicated azolectin liposomes (50 mg ml<sup>-1</sup>, 5 mM MES–Tris pH 7.4) resulting in a protein/lipid (w/w) ratio of 1/2000 to 1/4000. This mixture was diluted tenfold into patch clamp buffer and frozen in liquid nitrogen. The liposomes were thawed on ice, and 4% ethylene glycol was added. In an exsiccator, dehydration of 5 μl samples was performed over dry CaCl<sub>2</sub> for 1 h. Rehydration after addition of 10 μl patch clamp buffer to each sample was accomplished over night on glass plates in covered petri dishes.

### 2.7. Electrophysiology

Patch clamp techniques were applied to giant liposomes resuspended in the bath solution in the experimental chamber. Bath and pipette solution contained (in mM): 100 KCl and 5 MES–Tris adjusted to pH 7.4, or additionally, 1 CaCl<sub>2</sub> and 1 MgCl<sub>2</sub>. Test solutions were of identical composition or, according to the experimental conditions, additionally contained 0.01–10 mM K<sup>+</sup>-phosphate, 10 mM K<sup>+</sup>-sulfate, or 5 mM ADP adjusted to pH 7.4, respectively.

Micropipettes were produced from borosilicate glass with an internally fused filament providing quick-filling of the pipette from the back. The opening diameter of the tips was determined to be of around 500 nm (determined by scanning electron microscopy) displaying electrical resistances of 20–30 MΩ when filled with saline. Electrical signals were detected employing Ag/AgCl electrodes with a commercially available patch clamp amplifier (Axon Instruments, Axopatch 200A), digitized at 44 kHz (Instrutech, VR-10A) and stored on video tape. The

play-back signals were conditioned by an 8-pole Bessel low pass filter (Rockland System, 816) and the output fed into a computer for further analysis with pCLAMP software (Axon Instruments).

Test solutions were applied to excised patches via a perfusion system. The reference electrode was positioned in the stream of perfusion. Considering the giant liposomes as cells, inside-out configurations were used throughout. Their formation occurred spontaneously, or by short exposition ( $< 1$  s) of the pipette tip to air in those cases where a small vesicle had been excised from the giant liposome.

### 3. Results

#### 3.1. Purity of functional phosphate carrier

Phosphate carrier protein was solubilized from inclusion bodies using sodium lauroylsarcosinate [13,17]. Therefore, no contaminating mitochondrial membrane proteins, e.g., porin or any other channels of the inner and outer membrane, could be present. After solubilization of the functionally active protein, a subsequent chromatography on hydroxyapatite was necessary to obtain electrophysiologically detectable PIC. During this procedure, Triton X-100 in a buffer containing KCl,  $KP_i$ , DTE and cardiolipin was added. The recovery of total protein after elution of five fractions was about 30% but only about 20% in the absence of cardiolipin. The transport activity of the PIC before chromatography on hydroxyapatite was  $0.51 \pm 0.17 \text{ mmol min}^{-1} \text{ g}_{\text{protein}}^{-1}$ . After this chromatography, the specific transport rate increased up to three-fold. Proteoliposomes containing PIC from fractions 2 to 5 were converted into giant liposomes by a dehydration/rehydration cycle as described in Section 2. We have carried out transport measurements with exactly those proteoliposomes (fractions 2–5) used for generating giant liposomes. They were perfectly active, although the specific activity was somewhat higher with proteoliposomes in which the procedure originally optimized for phosphate transport had been used. In all experiments, a protein/phospholipid ratio between 1/2000 to 1/4000 (w/w) was used. To exclude a possible contamination by egg yolk proteins as utilized in preparations for tracer measurements, highly purified

soybean phosphatidylcholine was used for the preparation of giant liposomes that were subjected to patch clamp experiments. However, after reconstitution in egg yolk phospholipids no difference in the electrical behavior could be observed. Therefore, we conclude that the reconstituted PIC was in a functional state, in tracer transport as well as in electrophysiological measurements.

#### 3.2. Influence of detergents

Usually, non-ionic polyoxyethylene detergents with low critical micellar concentration are used for reconstitution of functionally active carrier proteins from mitochondria [22]. PIC reconstitution is normally carried out in the presence of Triton X-114 [5]. Despite effective removal of detergent during reconstitution by treatment with biobeads, residual detergent might be present in the proteoliposomes. It is known that several types of detergent are able to induce channel-like activity in artificial membranes, even when present in very low concentrations. Here, we used Triton X-100 and SLS because, in contrast to  $C_{12}E_8$  and Triton X-114, no channel-like behavior was induced by these detergents. This was validated by electrophysiological investigation of liposomes prepared in the absence of protein but in the presence of those detergents. As an alternative control, detergents were directly added to the bath solution (results not shown).

#### 3.3. Phosphate dependence of the channel

Undisputably, the proof for the function as an ion channel of the purified and reconstituted phosphate carrier would be given by channel-like current fluctuations recorded by patch clamp techniques, and a blocking effect of the substrate phosphate applied to the PIC channel, reverting the protein into carrier mode. Fig. 1 displays single channel recordings of the reconstituted PIC. Current fluctuations through the conductant protein occur at about 25 pS at both polarities of clamped voltage,  $\pm 80$  mV, in the absence of divalent cations (Fig. 1A). However, a marked current is passing the membrane patch at the apparent closed level which was not expected for seal resistances typically of a 50 G $\Omega$  range. Rather, a leak current of only about 1.5 pA or less should remain in the closed state at 80 mV. To rule out that

the reconstitution procedure itself yielded leaky vesicles, we carried out patch clamp experiments on liposomes that had not been doped with the protein. In these experiments, no significant leak current could be detected. Also, at the onset of seal formation on PIC-doped liposomes, when test pulses were applied through the opening of the patch pipette, the increased leak current did not become visible. Therefore, it has to be assumed that the channel may exist in a state of low conductance that hardly switched to a completely closed state. In panel B of Fig. 1, another trace recorded under the same experimental conditions as that shown in panel A but in the

presence of 10 mM phosphate, displays the occurrence of a closed state of  $-1.25$  pA that fits the expected leak current. The smallest conductance state in the absence of phosphate was  $-2.2$  pA (Fig. 1B). At positive clamp voltages, the recorded channel displayed markedly shorter dwell times in either open or closed state than it did at negative clamp voltages (cf. Fig. 1A).

The observed currents were blocked by 10 mM phosphate in either the presence or absence of divalent cations. The phosphate-induced block was fully reversible ( $n = 31$ ). In Fig. 2, the effect of 10 mM phosphate on single channel currents is shown in the

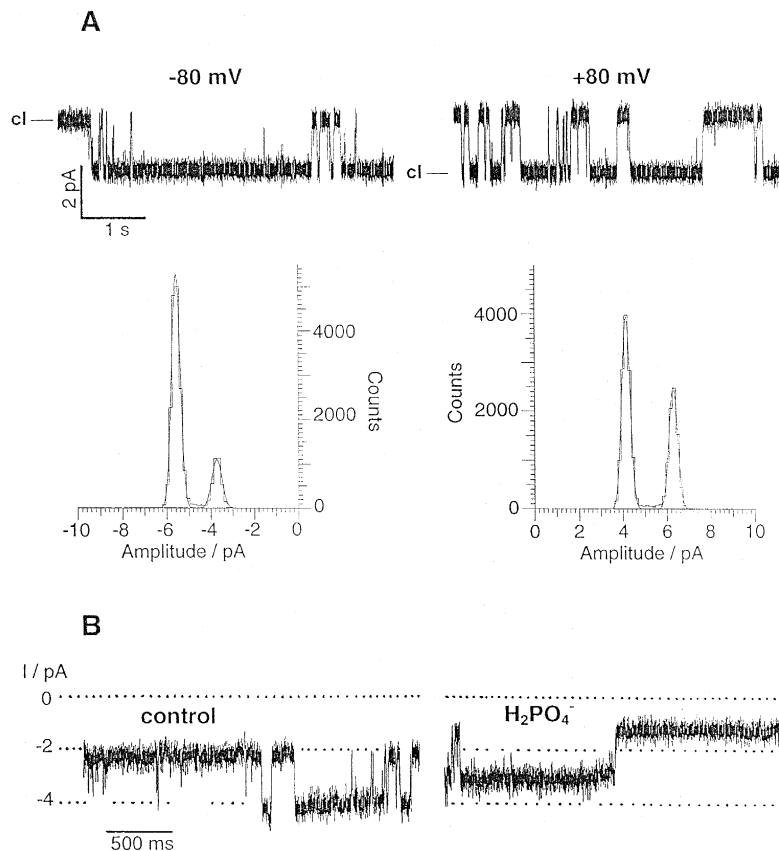


Fig. 1. Activity of a single PIC channel in excised patch configuration in the absence of divalent cations. (A) At  $-80$  mV clamp voltage, the channel displays current fluctuations from an apparent baseline of  $-3.7$  pA to an open level of  $-5.6$  pA (24 pS). At the right-hand side, a trace is shown where the channel fluctuates upward into the open state of  $6.3$  pA (27 pS) from an apparent closed level at  $4.1$  pA. At negative voltage ( $-80$  mV) dwell times of the open state as well as open probability are greater than at positive voltage ( $+80$  mV). (B) Recording of channel activity at  $-80$  mV on a different patch, but under the same experimental conditions as that in A. Likewise, in control solution the apparent closed level was at  $-2.2$  pA and the channel opened to  $-4$  pA (23 pS). However, when the patch was superfused with phosphate-containing solution, a baseline of smaller current ( $-1.25$  pA) was reached which was identical to the leak current at the time of seal formation. The amplitude of current fluctuations was retained during the first few seconds, then, the channel did not show open events furthermore. Experimental solutions (in mM): 100 KCl, 5 MES-Tris, adjusted to pH 7.4. Control and pipette solutions were identical. Signal conditioning: 8-pole Bessel filter set to 2 kHz.

presence of  $\text{Ca}^{2+}$  and  $\text{Mg}^{2+}$ . As in most recordings, the apparent closed level was above the expected one in control solution (i.e., without phosphate). Three conductance states of 4, 13 and 36 pS, respectively, on top of the apparent baseline ( $-5.73$  pA) were observed. In this patch, the channel current could not be completely blocked by phosphate, but the apparent closed level at  $-4.6$  pA was below that one observed under control conditions. After wash-out, the previously detected baseline at  $-5.73$  pA reappeared. Also, conductant states similar in amplitude to those recorded before phosphate treatment became again evident (4, 19, and 41 pS, respectively). Interestingly, the dwell time of the high conducting state was considerably increased.

Fig. 3 displays the effects upon PIC channel activity of different phosphate concentrations applied to the same patch. Compared to control conditions (without phosphate), 10  $\mu\text{M}$  phosphate did not alter channel behavior, whereas 100  $\mu\text{M}$  and 1 mM phosphate induced new fluctuation levels of increased amplitude. Particularly, on application of 1 mM phosphate, a maximum current amplitude appeared which was almost twice that found under control condition (detected in 12 of 18 experiments). Again, 10 mM phosphate almost completely blocked channel activity. Referring to the blocked state as induced by 10 mM phosphate, the following current levels of the open channel that existed at several conditions applied were detected:  $-1.7 \pm 0.3$  pA corresponding to 21 pS (in solutions: control, 10  $\mu\text{M}$ , 1 mM, 10 mM phosphate),  $-2.7 \pm 0.2$  pA corresponding to 34 pS (control; 10  $\mu\text{M}$ , 100  $\mu\text{M}$ , 1 mM phosphate),  $-3.9 \pm 0.2$  pA corresponding to 49 pS (control; 10, 100  $\mu\text{M}$  phosphate). Two higher current levels became visible at 100  $\mu\text{M}$  ( $-4.9$  pA, 61 pS) and 1 mM ( $-6.8$  pA, 85 pS) phosphate. Noticeably, phosphate concentrations equal to or greater than 100  $\mu\text{M}$  increased the current noise markedly.

### 3.4. Block specificity and anion specificity

To characterize the PIC protein with regard to its anion selectivity, different anions were applied to the PIC channel. A possible specificity of blockade by divalent anions was examined by adding sulfate (10 mM), vanadate (10 mM), and ADP (5 mM), respectively, to the control solution. The selectivities were

determined by subsequently changing the solutions, beginning with control, then a solution containing the test ion, eventually to phosphate containing medium. Sulfate is structurally related to phosphate, whereas ADP possesses similar properties as phosphate in terms of Lewis base characteristics. None of those anions induced a block of the channel similar to that

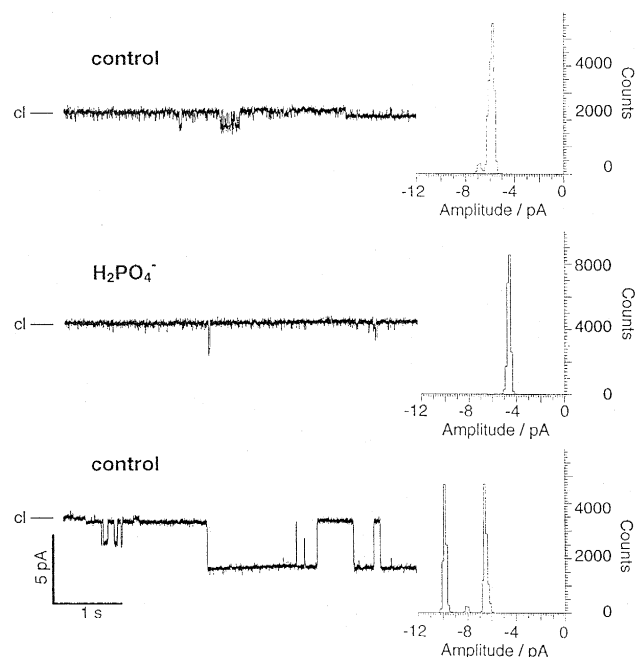


Fig. 2. Suppression of PIC channel activity in the presence of phosphate in the test solution. An excised patch exhibiting single channel activity was subsequently exposed to control solution (without phosphate), phosphate-containing solution, and again control solution, respectively. The initial current fluctuations of  $-0.34$  and  $-1.11$  pA amplitudes, respectively, were almost completely abolished by the test solution containing 10 mM phosphate. The previous baseline dropped from  $-5.73$  to  $-4.59$  pA. After wash-out with phosphate-free control solution, a baseline of  $-6.16$  pA was determined, and the channel conductance increased. Current amplitudes of fluctuations into an open state then amounted to  $-0.35$  pA, a value corresponding to that previously detected,  $-1.52$  and  $-3.3$  pA, respectively. Mean values of those various current levels are displayed in the respective all-point amplitude histograms adjacent to the traces. The apparent closed states are indicated left-hand side of the traces. Note that, due to rare occurrence or short lifetime, histogram peaks being ascribed to those events will elevate only slightly above the abscissa. Experimental solutions (in mM): 100 KCl, 1  $\text{CaCl}_2$ , 1  $\text{MgCl}_2$ ,  $\pm 10$   $\text{K}_2\text{H}/\text{KH}_2\text{PO}_4$ , 5 MES-Tris, adjusted to pH 7.4. Control and pipette solutions were identical and did not contain phosphate. Clamp voltage  $-80$  mV. Signal conditioning: 8-pole Bessel filter set to 2 kHz.

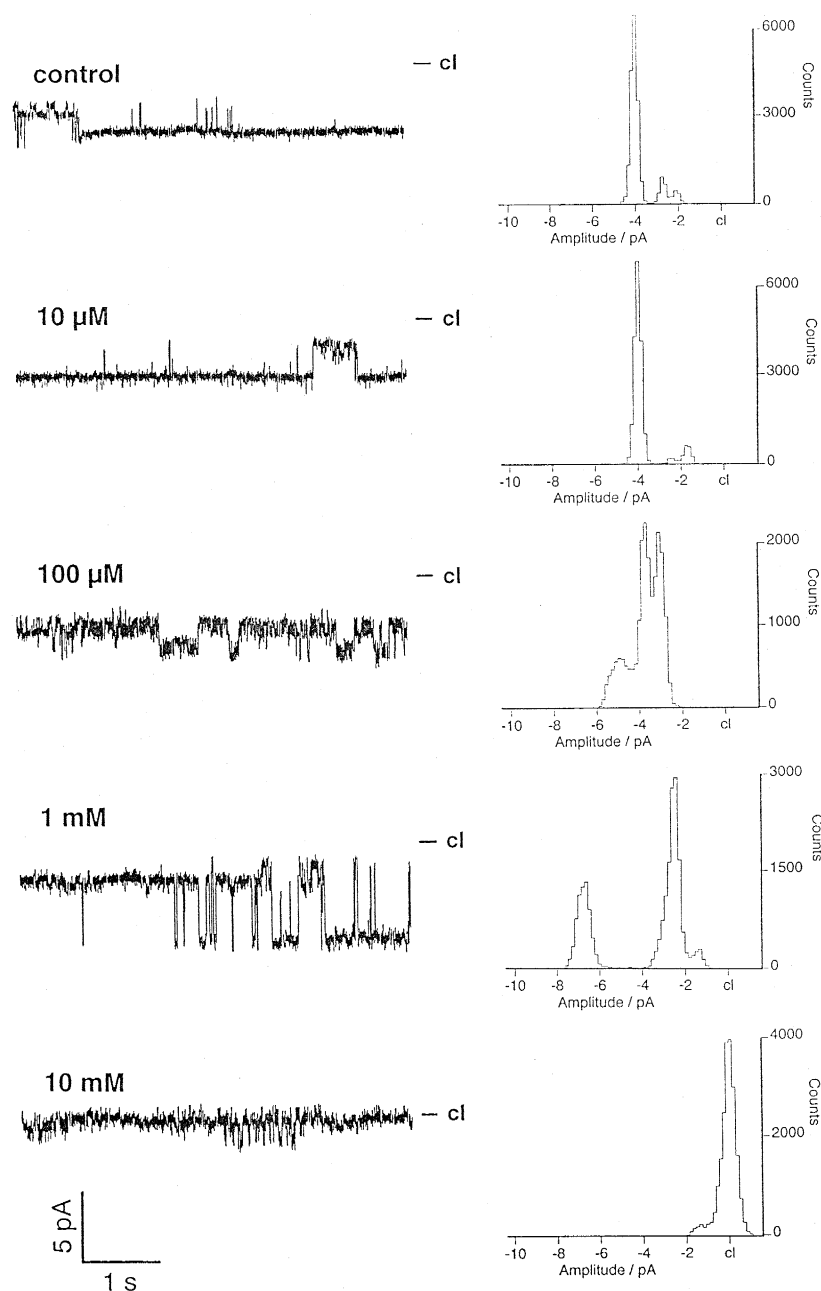


Fig. 3. Effect of different phosphate concentrations on PIC single channel activity. Left-hand side, original traces are shown. The respective phosphate concentrations applied are indicated and the closed level is marked (determined to be the blocked state at 10 mM phosphate). Right-hand side, the corresponding amplitude histograms are given to allow a comparison of current levels in the channel open states. At all conditions except that of 100  $\mu\text{M}$  phosphate, channel current of  $-1.7$  pA appeared, similarly, another level of  $-2.7$  pA became always visible, except at 10 mM phosphate. A third current level of  $-3.9$  pA reappeared at superfusion of control, 10  $\mu\text{M}$  and 100  $\mu\text{M}$  phosphate solutions. Finally, current fluctuations to  $-4.9$  and  $-6.8$  pA occurred at 100  $\mu\text{M}$  and 1 mM phosphate, respectively. Experimental solutions (in mM): 100 mM KCl, 1  $\text{CaCl}_2$ , 1  $\text{MgCl}_2$ ,  $\pm \text{K}_2\text{H/KH}_2\text{PO}_4$ , 5 MES-Tris, adjusted to pH 7.4. Control solution and pipette filling solution were identical. Clamp voltage:  $-80$  mV. Signal conditioning: 8-pole Bessel filter set to 2 kHz.

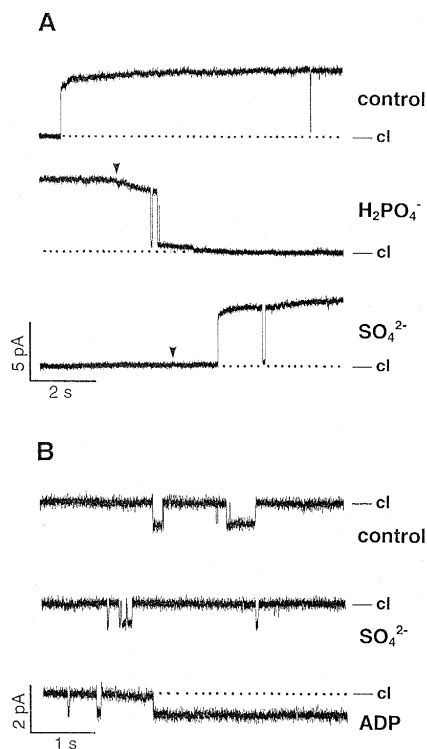


Fig. 4. Specificity of PIC channel blockade towards phosphate. The apparent closed states are indicated right-hand side at each trace. (A) Superfusion of the excised patch with 10 mM phosphate (arrow-head) induced channel blockade, at the onset of wash-out (arrow-head) with control solution containing 10 mM sulfate, the channel resumed activity. The amplitudes of current fluctuations before phosphate application and during sulfate washout were identical. (B) Recording of a different patch. At either condition, the current through the PIC channel was not altered in control solution (without phosphate, sulfate or ADP), 10 mM sulfate, or 5 mM ADP, respectively. Experimental solutions (in mM): 100 KCl, 1  $\text{CaCl}_2$ , 1  $\text{MgCl}_2$ ,  $\pm 10$   $\text{K}_2\text{H}/\text{KH}_2\text{PO}_4$ ,  $\pm 10$   $\text{K}_2\text{SO}_4$ ,  $\pm 5$  ADP, 5 MES-Tris, pH adjusted to 7.4. Control and pipette solution were symmetrical. Clamp voltage: +80 mV (A), –60 mV (B). Signal conditioning: 8-pole Bessel filter set to 1 kHz.

observed in the presence of 10 mM phosphate (Fig. 4). Fig. 4A displays the blockade of the channel by 10 mM phosphate which was abolished immediately after perfusion with sulfate solution. The current amplitude in sulfate solution was the same as that in control solution. In Fig. 4B, another experiment is shown where the control solution had been exchanged successively for sulfate (10 mM) and ADP (5 mM), respectively. In both experiments, the ampli-

tude of current fluctuations remained unchanged. Also in the case of 10 mM vanadate, the current amplitudes were not affected, however, dwell times in either state were decreased (traces not shown).

To determine the ion species transported through the PIC channel, namely whether it is an anion or cation, we applied a gradient of 10-fold KCl concentration over the excised membrane patch. The inside-out configuration was achieved in symmetrical solutions of 100 mM KCl after elimination of the electrode offset voltage. When superfusing the patch with 10 mM KCl, a leak current developed according to the potential difference generated by the  $\text{Cl}^-$  gradient at the reference electrode. The electrical  $\text{Cl}^-$ -dependent gradient amounted to 52 mV (calculated from Nernst's equation). If the channel were either cation or anion specific, negative or positive current fluctuations, respectively, were expected. At a pipette clamp voltage of 0 mV, we observed positive current fluctuations. The amplitude of those fluctuations corresponded to the driving force of  $\text{Cl}^-$  ions directed from the pipette interior to the bath solution (traces not shown). Assuming that the single channel observed in this experiment has also a conductance of 40 pS (determined as the mean value from all measurements), the actual driving force across the patch were calculated to be 105 mV. An explanation for this voltage is given by the fact that both, the potential difference generated at the electrode surface, and the concentration gradient across the patch, added up to a final driving force of 105 mV. The amplitude of those current fluctuations of 4.2 pA which corresponded to this driving force and was caused by the concentration gradient strongly suggests a strict selectivity towards anions, i.e.,  $\text{Cl}^-$ .

### 3.5. Current–voltage relationship

To further characterize the electrical PIC channel properties, the voltage dependency of this channel was measured in the presence and absence of 10 mM phosphate, respectively. In Fig. 5, current–voltage curves are depicted that were generated by applying voltage ramps of  $\pm 180$  mV (Fig. 5A–B;  $-\text{Ca}^{2+}$  and  $\text{Mg}^{2+}$ ) or  $\pm 160$  mV (Fig. 5C–D;  $+\text{Ca}^{2+}$  and  $\text{Mg}^{2+}$ ) to the excised patch. The baseline was obtained by subtracting current traces at times where the channel



was inactive from traces where channel activity was observed. In the presence of phosphate, channel conductance was reduced from 41 pS to 19 pS (inwardly directed current).  $\text{Ca}^{2+}$  and  $\text{Mg}^{2+}$  ions in the test solution were found to enhance the inhibitory effect of phosphate, the channel conductance changed from 50 to 12 pS (inwardly directed current) under these conditions. In both experiments,  $I$ – $V$  curves display slightly inward-rectifying behavior under control conditions, i.e., without divalent cations. The attenuation factor was 0.83 in the absence, and 0.56 in the presence of divalent cations, when comparing outward to inward conductances. As shown in Fig. 3, also in this case the noise was increasing after phosphate application. In Fig. 5C, a second channel becomes active during opening of a first channel, displaying the same conductance. The increased noise in Fig. 5C is due to the combination in the graph of two different traces recorded on the same patch, one of which showed channel activity in inward direction, the other one outwardly directed current fluctuations.

### 3.6. Effects of divalent cations

As shown before, voltage exerts influence on PIC channel gating (cf. Fig. 1). To examine another possible regulatory mechanism, we measured PIC channel activity in the presence and absence, respectively, of divalent cations. In Fig. 6, the effect of divalent cations upon the PIC-channel activity is shown. The pipette solution did not contain divalent cations. In the presence of  $\text{Ca}^{2+}$  and  $\text{Mg}^{2+}$  the channel was mainly dwelling in the closed state at  $-0.8$  pA, switching to an open level of  $-1.8$  pA that corresponded to a conductance of 12.5 pS. Open and close dwell times were of seconds range in the presence of divalent cations. After wash-out of divalent cations a new apparent closed state at about  $-3.5$  pA was observed. From this level the channel fluctuated between this closed state and an open state of  $-6.3$  pA

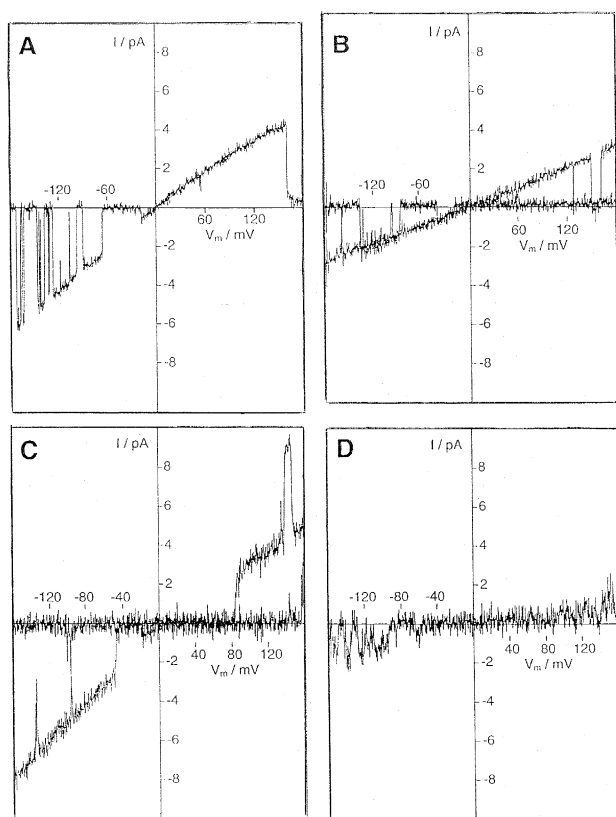


Fig. 5. Current voltage relations in the PIC channel in the absence (A, B) or presence (C, D) of divalent cations, respectively. (A) Voltage ramps were applied to an excised patch during superfusion with control solution. The  $I$ – $V$  curve was obtained by subtracting a trace showing no channel activity from another one that exhibited current fluctuations. The maximum conductance of the channel was 41 pS in inward current direction. The channel displayed a slight attenuation of outward current. (B)  $I$ – $V$  curve recorded on the same patch during 10 mM phosphate superfusion. The conductance had decreased to 20 pS, over the whole current range, no rectification occurred. Due to the rare opening events in the presence of phosphate, this curve was constructed by superimposing two traces showing activity, after subtraction of the leak current. (C)  $I$ – $V$  curve recorded from another patch. Two traces displaying channel activity at negative and positive clamp voltage were superimposed. Channel conductance amounted to 31 pS at negative voltage range. Also in this experiment, the channel displayed a slight inward rectification. During application of positive voltage, two channels exhibited activity simultaneously. (D)  $I$ – $V$  curve obtained on the same patch as in C after application of 10 mM phosphate. The conductance of the open channel had decreased to 10 pS at negative clamp voltages. Experimental solutions (in mM): 100 KCl, 1  $\text{CaCl}_2$  and 1  $\text{MgCl}_2$  (only in C and D),  $\pm 10$   $\text{K}_2\text{H/KH}_2\text{PO}_4$ , 5 MES–Tris, adjusted to pH 7.4. Pipette solutions and control solutions were symmetrical in the respective experiments ( $\pm$  divalent cations). Signal conditioning: 8-pole Bessel filter set to 1 kHz (A, B) or 2 kHz (C, D). Applied voltage ramps:  $\pm 180$  mV in A, B;  $\pm 160$  mV in C, D. Data points were sampled at a rate of 100 Hz (A, B) or 4 kHz (C, D), respectively.

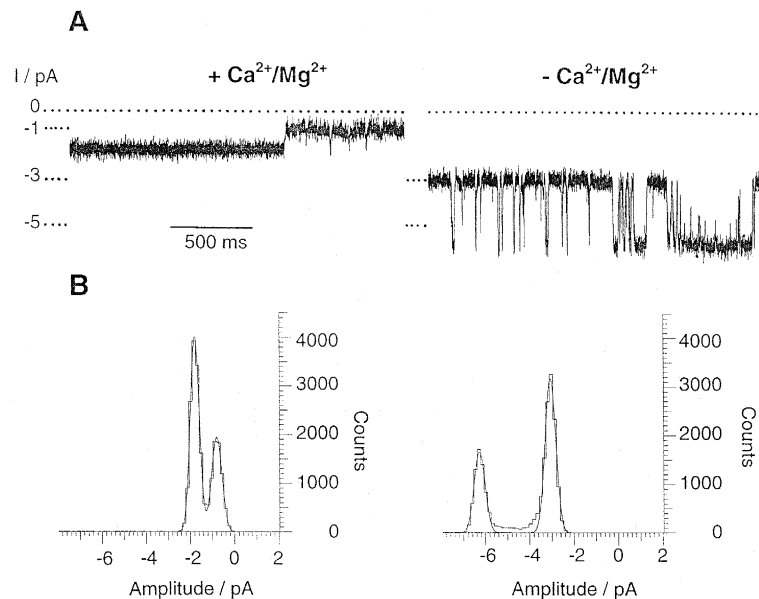


Fig. 6. Effect of divalent cations upon PIC channel activity. (A) In the presence of divalent cations (left-hand side), the channel exhibited its closed state at  $-0.8$  pA, and opened to  $-1.8$  pA (12.5 pS). Dwell times in either state are of seconds range. After superfusion of the excised patch with divalent cation-free solution (right-hand side), the observed closed level shifted to  $-3.5$  pA and fluctuations of increased amplitude ( $-6.3$  pA, 40 pS) but significantly shortened dwell times could be detected. (B) Amplitude histograms of the respective recordings shown in A. Experimental solutions (in mM): 100 KCl,  $\pm 1$  CaCl<sub>2</sub> and 1 MgCl<sub>2</sub>, 5 MES-Tris, pH adjusted to 7.4. Control solution and pipette solution (without divalent cations) were identical. Clamp voltage:  $-80$  mV. Signal conditioning: 8-pole Bessel filter set to 2 kHz.

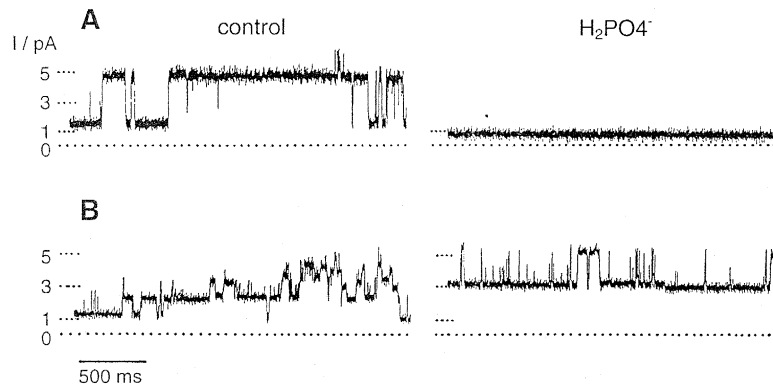


Fig. 7. Phosphate effects on PIC channels in giant liposomes prepared from sonicated proteoliposomes. (A) Current through a PIC channel in control medium (without phosphate) fluctuating between 1.2 pA (closed state) and 4.8 pA (open state, 45 pS). After superfusion of the excised patch with 10 mM phosphate, channel activity was completely suppressed. (B) Measurement on a different excised patch. After changing the superfusion from control to phosphate solution, the observed current fluctuations significantly altered characteristics. While a number of subconductant levels can be discerned under control conditions (closed state: 1.1 pA, open states: 2.42, 3.69, 4.83, and 5.66 pA; distances between the detected levels 10.5–16 pS), they were abolished under the regime of 10 mM phosphate, instead, uniform current fluctuations of increased amplitude (2.6 pA, 32 pS) appeared. Also, the baseline had shifted to an apparent closed state of 3.5 pA. This variation of channel behavior is opposite to all measurements carried out on preparations that did not include sonication. Experimental solution (in mM): 100 KCl, 1 CaCl<sub>2</sub>, 1 MgCl<sub>2</sub>,  $\pm$  K<sub>2</sub>H/KH<sub>2</sub>PO<sub>4</sub>, 5 MES-Tris, pH adjusted to 7.4. Control and pipette solution were identical. Clamp voltage:  $+80$  mV. Signal conditioning: 8-pole Bessel filter set to 1 kHz.

(40 pS). Open dwell times of the open state varied between  $< 1$  ms and 1 s (Fig. 6A). Again, an increased activity of the channel could be observed in the absence of  $\text{Ca}^{2+}$  and  $\text{Mg}^{2+}$ . As found in general, noise increased in the absence of divalent cations compared to measurements in the presence of  $\text{Ca}^{2+}$  and  $\text{Mg}^{2+}$  in the pipette solution (cf. Fig. 3). Fig. 6B shows all-points amplitude histograms constructed for either condition.

During measurements of PIC single channel activity in solutions without divalent cations, we repeatedly observed inactivation of the channel after exposure of the excised patch beyond several minutes, sometimes even earlier.

### 3.7. Channel orientation in the membrane

In another set of experiments, giant liposomes were formed using proteoliposomes that were subjected to an additional freeze–thaw–sonication step (cf. Fig. 7). We expected a random orientation of the PIC protein after this treatment [5]. In 9 experiments from a total of  $n = 21$ , we found inhibition by 10 mM phosphate of the PIC channel, when employing these giant liposomes. Surprisingly, in the remaining 12 experiments phosphate not only was inefficient as a blocker, rather current fluctuations through the PIC channel exhibited an increased and uniform amplitude. These results suggest that the orientation of the PIC channel was random in those sonicated proteoliposomes, and also that the initial orientation is maintained during the formation of giant liposomes. On the other hand, the blocking efficiency of phosphate in almost all experiments where the additional sonication was omitted points to a preferential orientation of the protein. Fig. 7A shows cessation of current fluctuations upon phosphate treatment. At a clamp voltage of +80 mV, the current amplitude observed at control condition (without phosphate) was uniformly 3.6 pA (45 pS) with a baseline at 1.2 pA. Application of 10 mM phosphate induced a baseline shift to 0.6 pA, and channel current was suppressed. On a PIC channel that presumably was inversely oriented (Fig. 7B), several almost equidistant conductance levels were recorded ( $14.2 \pm 2.1$  pS, +80 mV clamp voltage) under control conditions (without phosphate). The baseline, previously at 1.1 pA, was shifted to a level of 3.5 pA by 10 mM

phosphate. The initial 14.2 pS fluctuations completely disappeared and uniform current fluctuations of 32 pS occurred. It is noteworthy that this increased conductance could not be detected during control condition. It has, therefore, to be concluded that the PIC channel had changed its characteristics upon phosphate treatment. Consequently, the ensemble of all 14.2 pS conductance states, observed under control conditions, must be interpreted as subconductances of a single PIC channel.

## 4. Discussion

For both [ $^{33}\text{P}$ ]phosphate exchange and patch clamp experiments on giant liposomes, heterologously expressed phosphate carrier protein (PIC) was utilized. In *E. coli*, overexpression of the recombinant PIC protein led to formation of inclusion bodies which could easily be isolated. Utilization of those inclusion bodies and the subsequent steps of purification excluded a contamination by other mitochondrial membrane proteins. The isolation led to a highly purified protein showing a single band in SDS–PAGE at 32 kDa [18]. With respect to electrophysiological studies, this is the first report on utilization of a heterologously expressed protein of the mitochondrial inner membrane. Tracer measurements revealed a transport rate of about  $120 \text{ mmol min}^{-1} \text{ g}_{\text{protein}}^{-1}$  through the PIC protein [18]. This corresponds to a current of  $2 \times 10^{-17}$  amperes carried by a single phosphate carrier dimer with an apparent molecular mass of 64 kDa. Currents of that size cannot be detected by electrophysiological techniques, however, it turned out that a single functional PIC was able to mediate a current of more than five magnitudes greater than that calculated from tracer experiments.

The PIC protein used in these experiments was functionally active in phosphate/phosphate exchange experiments. The specific transport rates determined were lower than those previously reported. This was due to optimizing the purification and reconstitution procedure for the electrophysiological measurements. In addition to the transport modes ( $\text{P}_i/\text{P}_i$  exchange,  $\text{P}_i/\text{OH}$  exchange, unidirectional transport of  $\text{P}_i$  after  $\text{HgCl}_2$  treatment), a fourth mode of function could be ascribed to the PIC, namely that of an anion channel.

The PIC channel displayed a number of conductance states with that of  $40 \pm 10$  pS as the most frequent one (depending on the absence or presence of divalent cations, see Fig. 1). Application of 10 mM phosphate to an excised patch resulted in closing of the channel which was, however, reversible after washing the patch with control solution. This phosphate-dependent channel blockade was specific, since other anions like sulfate, vanadate or ADP did not induce any similar effect (Fig. 4). Furthermore, the PIC channel exhibited a graded response to increasing phosphate concentrations. The effects of phosphate as the actual substrate of the PIC, seen in a concentration-dependent way as a stimulation and a blockade, respectively, cannot be explained conclusively (Fig. 3). It could, however, be characteristic of a phosphate-dependent conformational change of the PIC protein.

A modifiable protein conformation is also indicated by a conductance decrease and prolongation of open/closed dwell times, respectively, in the presence of 1 mM  $\text{Ca}^{2+}$  and  $\text{Mg}^{2+}$  (Fig. 6). Furthermore, an almost permanent open state in the absence of divalent cations of the range of 15 pS that was hardly eliminated even by 10 mM phosphate, was also reduced in the presence of divalent cations. This reduction (cf. Fig. 6) is also revealed in  $I$ – $V$  relationships depicted in Fig. 5, where the channel retains a low conducting state of 12 to 19 pS (presence or absence of divalent cations, respectively). Besides, the channel conductance displayed a slight voltage dependent rectification that is not seen in the presence of phosphate. Therefore, a regulatory function of divalent cations on PIC is conceivable.

The orientation of the PIC appeared to be random in sonicated proteoliposomal preparations whereas a preferentially asymmetric orientation was assumed in non-sonicated preparations (cf. [7]) and maintained during conversion of the proteoliposomes into giant liposomes. Since it is known for homologous phosphate exchange in tracer measurements that the  $K_m$  of the internal and external  $\text{P}_i$  binding sites are 9 and 1.2 mM, respectively [18], our results strongly suggest that in excised patches the PIC exposed its matrix face to the test solutions, because significant blockade by phosphate could only be observed in ‘inside-out’ configuration at concentrations as high as 10 mM.

The present electrophysiological investigation into PIC characteristics puts this transport protein in a line with others belonging to the family of mitochondrial inner membrane transporters, with respect to their capability to switch between carrier and channel mode of action. Recently, the nucleotide carrier from bovine heart mitochondria, and the uncoupling protein from brown adipose tissue mitochondria, were reported to show channel-like activity under similar experimental conditions as those employed for the phosphate carrier in this work [9,10]. The reconstituted nucleotide carrier (AAC) exhibits channel activity which strictly depended on the presence of  $\text{Ca}^{2+}$  and could be blocked by bongkrekate, a specific inhibitor of the AAC. The AAC channel was found to be slightly selective towards cations. The uncoupling protein (UCP), like PIC, mediates a  $\text{Cl}^-$  current with a conductance of 75 pS that could be blocked by nucleotides. Functioning as a channel, both proteins, the AAC and the UCP, translocate substrates different from those that are transported in their original carrier mode. It has been suggested [9] that the AAC is identical to the previously reported mitochondrial permeability transition pore [23], mitochondrial multiple conductance channel [24] or mega-channel [25], the physiological relevance of the channel mode of the UCP is still obscure.

The phosphate/triose phosphate carrier of chloroplasts was characterized to be able to function in a channel-like behavior at high  $\text{Cl}^-$  or phosphate concentrations. However, unlike mitochondrial carriers (PIC, AAC, UCP), these ions also represent the substrates of the protein’s carrier function when applied in concentrations below 100 mM [11].

In situ electrophysiological recordings of the inner mitochondrial membrane revealed several anion-selective channels [26]. None of those channels has been purified or sequenced, to date. Therefore, their characterization is restricted to electrophysiological experiments. The so-called ‘centum picosiemens’ channel detected in mammalian mitochondria appears to be negatively regulated by  $\text{Ca}^{2+}$ , similar to the PIC protein, but its conductance of about 107 pS exceeds that of the PIC [27,28]. Furthermore, an ‘intermediate’ and a ‘small mitochondrial anion channel’ (INMAC, SMAC) were described [29,30], exhibiting conductances similar to those depicted for the PIC in this work. In contrast to the PIC channel, divalent

cations stimulate activity of the INMAC and SMAC, respectively. This enhancement was suggested to be due to a modification of surface charges at the channel gate, because the amplitude of current fluctuations remained constant. The authors suggested that SMAC could represent a portion of the presumptively disrupted INMAC, produced by sonication of their preparation [29,30].

Two  $\text{Cl}^-$  channels that are ATP-dependent have been found in yeast mitochondria [31]. They display different conductances of 45 and 400–800 pS. The channel exhibiting the smaller conductance would correlate with the PIC channel, however, its  $\text{Ca}^{2+}$  and  $\text{Mg}^{2+}$  insensitivity contradicts a supposable identity to PIC. In excised patches drawn from mitoplast membranes, an ‘alkali-activated channel’ was triggered upon superfusion with a solution of alkaline pH. Its conductance amounted to 45 pS [32]. In contrast, the PIC channel is active at neutral pH.

Another channel, observed in the mitochondrial inner membrane (IMAC) is conducting a large variety of anions, e.g.,  $\text{Cl}^-$  and  $\text{ATP}^{4-}$ , with a conductance similar to that which was observed here for the PIC [33,34]. Interestingly, IMAC activity could be enhanced by application of 9 mM phosphate to the cytosolic side at pH 7.4 [35]. These results are corresponding to our experiments on sonicated preparations, where 10 mM phosphate induced a stimulation of the PIC channel that presumably was oriented with its cytosolic face towards the phosphate-containing solution. Furthermore, the IMAC responds to thiol-modifying substances like mersalylic acid, which also exerted influence on the phosphate carrier as shown in tracer experiments [5,34,36]. Eventually, an inhibition of IMAC by  $\text{Mg}^{2+}$  was observed [34] that was also detected in PIC, though, in the latter case, a combination of  $\text{Ca}^{2+}$  and  $\text{Mg}^{2+}$  had been applied. Although these coincidental results point at an identity between the IMAC and the PIC, more data are necessary to prove this assumption.

## Acknowledgements

We are grateful to D. Paine for providing us with the plasmid pNHYM131, to H. Wohlrab for help in the heterologous expression of the PIC, and to H. Sahm and U.B. Kaupp for continuous and generous

support. This work was financially supported by the Deutsche Forschungsgemeinschaft (SFB 189) and the Fonds der Chemischen Industrie.

## References

- [1] K.F. LaNoue, A.C. Schoolwerth, in: L. Ernster (Ed.), *Bioenergetics*, Elsevier, Amsterdam, 1984, pp. 221–268.
- [2] R. Krämer, F. Palmieri, in: L. Ernster (Ed.), *Molecular Mechanisms in Bioenergetics*, Elsevier, Amsterdam, 1992, pp. 359–384.
- [3] H. Wohlrab, *Biochim. Biophys. Acta* 853 (1986) 115–134.
- [4] J.P. Wehrle, P.L. Pedersen, *J. Membrane Biol.* 111 (1989) 199–213.
- [5] R. Stappen, R. Krämer, *Biochim. Biophys. Acta* 1149 (1993) 40–48.
- [6] T. Dierks, A. Salentin, C. Heberger, R. Krämer, *Biochim. Biophys. Acta* 1028 (1990) 268–280.
- [7] C. Indiveri, A. Tonazzi, F. Palmieri, *Biochim. Biophys. Acta* 1069 (1991) 110–116.
- [8] F. Palmieri, G. Prezioso, F. Bisaccia, C. Indiveri, V. Zara, V. De Pinto, G. Genchi, *Adv. Myochem.* 1 (1987) 87–104.
- [9] N. Brustovetsky, M. Klingenberg, *Biochemistry* 35 (1996) 8483–8488.
- [10] S.G. Huang, M. Klingenberg, *Biochemistry* (1996) in press.
- [11] M. Schwarz, A. Gross, T. Steinkamp, U.I. Flügge, R. Wagner, *J. Biol. Chem.* 269 (1994) 29481–29489.
- [12] H. Murakami, G. Blobel, D. Pain, *Proc. Natl. Acad. Sci. USA* 90 (1993) 3358–3362.
- [13] H. Wohlrab, C. Briggs, *Biochemistry* 33 (1994) 9371–9375.
- [14] W. Hanke, W.R. Schlue, *Planar Lipid Bilayers*, Academic Press, London, 1993, p. 47.
- [15] A. Phelps, H. Wohlrab, *J. Biol. Chem.* 266 (1991) 19882–19885.
- [16] D. Pain, H. Murakami, G. Blobel, *Nature* 347 (1990) 444–449.
- [17] G. Fiermonte, J.E. Walker, F. Palmieri, *Biochem. J.* 294 (1993) 293–299.
- [18] A. Schroers, R. Krämer, H. Wohlrab, *J. Biol. Chem.* (1997) in press.
- [19] J.R. Dulle, P.A. Grieve, *Anal. Biochem.* 64 (1975) 136–141.
- [20] G.L. Peterson, *Anal. Biochem.* 83 (1977) 346–356.
- [21] M. Criado, B.U. Keller, *FEBS Lett.* 224 (1987) 172–176.
- [22] R. Krämer, F. Palmieri, *Biochim. Biophys. Acta* 974 (1989) 1–32.
- [23] D.R. Hunter, R.A. Haworth, *Arch. Biochem. Biophys.* 195 (1979) 453–459.
- [24] K.W. Kinnally, M.L. Campo, H.T. Tedeschi, *J. Bioenerg. Biomembr.* 21 (1989) 497–506.
- [25] V. Petronilli, I. Szabó, M. Zoratti, *FEBS Lett.* 259 (1989) 137–143.
- [26] M. Zoratti, I. Szabó, *J. Bioenerg. Biomembr.* 26 (1994) 543–553.

- [27] K.W. Kinnally, D.B. Zorov, Y.N. Antonenko, S. Perini, *Biochem. Biophys. Res. Comm.* 176 (1991) 1183–1188.
- [28] M.C. Sorgato, B.U. Keller, W. Stühmer, *Nature* 330 (1987) 498–500.
- [29] K.A. Hayman, R.H. Ashley, *J. Membr. Biol.* 136 (1993) 191–197.
- [30] K.A. Hayman, T.D. Spurway, R.H. Ashley, *J. Membr. Biol.* 136 (1993) 181–190.
- [31] C. Ballarin, M.C. Sorgato, *J. Bioenerg. Biomembr.* 28 (1996) 125–130.
- [32] Y.N. Antonenko, D. Smith, K.W. Kinnally, H. Tedeschi, *Biochim. Biophys. Acta* 1194 (1994) 247–254.
- [33] T. Klitsch, D. Siemen, *J. Membr. Biol.* 122 (1991) 69–75.
- [34] A.D. Beavis, *J. Bioenerg. Biomembr.* 24 (1992) 77–90.
- [35] L.T. Ng, M.J. Selwyn, H.L. Choo, *Biochim. Biophys. Acta* 1183 (1993) 180–184.
- [36] A.D. Beavis, H. Davatol-Hag, *J. Bioenerg. Biomembr.* 26 (1996) 207–214.